Fermilab-Pub-05/217-E

Measurement of the $t\bar{t}$ Production Cross Section in $p\bar{p}$ Collisions at $\sqrt{s} = 1.96$ TeV in Dilepton Final States

V.M. Abazov,[35] B. Abbott,[72] M. Abolins,[63] B.S. Acharya,[29] M. Adams,[50] T. Adams,[48] M. Agelou,[18] J.-L. Agram,[19] S.H. Ahn,[31] M. Ahsan,[57] G.D. Alexeev,[35] G. Alkhazov,[39] A. Alton,[62] G. Alverson,[61] G.A. Alves,[2] M. Anastasoaie,[34] T. Andeen,[52] S. Anderson,[44] B. Andrieu,[17] Y. Arnoud,[14] A. Askew,[48] B. Åsman,[40] A.C.S. Assis Jesus,[3] O. Atramentov,[55] C. Autermann,[21] C. Avila,[8] F. Badaud,[13] A. Baden,[59] B. Baldin,[49] P.W. Balm,[33] S. Banerjee,[29] E. Barberis,[61] P. Bargassa,[76] P. Baringer,[56] C. Barnes,[42] J. Barreto,[2] J.F. Bartlett,[49] U. Bassler,[17] D. Bauer,[53] A. Bean,[56] S. Beauceron,[17] M. Begalli,[3] M. Begel,[68] A. Bellavance,[65] S.B. Beri,[27] G. Bernardi,[17] R. Bernhard,[49,*] I. Bertram,[41] M. Besançon,[18] R. Beuselinck,[42] V.A. Bezzubov,[38] P.C. Bhat,[49] V. Bhatnagar,[27] M. Binder,[25] C. Biscarat,[41] K.M. Black,[60] I. Blackler,[42] G. Blazey,[51] F. Blekman,[42] S. Blessing,[48] D. Bloch,[19] U. Blumenschein,[23] A. Boehnlein,[49] O. Boeriu,[54] T.A. Bolton,[57] F. Borcherding,[49] G. Borissov,[41] K. Bos,[33] T. Bose,[67] A. Brandt,[74] R. Brock,[63] G. Brooijmans,[67] A. Bross,[49] N.J. Buchanan,[48] D. Buchholz,[52] M. Buehler,[50] V. Buescher,[23] S. Burdin,[49] S. Burke,[44] T.H. Burnett,[78] E. Busato,[17] C.P. Buszello,[42] J.M. Butler,[60] J. Cammin,[68] S. Caron,[33] W. Carvalho,[3] B.C.K. Casey,[73] N.M. Cason,[54] H. Castilla-Valdez,[32] S. Chakrabarti,[29] D. Chakraborty,[51] K.M. Chan,[68] A. Chandra,[29] D. Chapin,[73] F. Charles,[19] E. Cheu,[44] D.K. Cho,[60] S. Choi,[47] B. Choudhary,[28] T. Christiansen,[25] L. Christofek,[56] D. Claes,[65] B. Clément,[19] C. Clément,[40] Y. Coadou,[5] M. Cooke,[76] W.E. Cooper,[49] D. Coppage,[56] M. Corcoran,[76] A. Cothenet,[15] M.-C. Cousinou,[15] B. Cox,[43] S. Crépé-Renaudin,[14] D. Cutts,[73] H. da Motta,[2] M. Das,[58] B. Davies,[41] G. Davies,[42] G.A. Davis,[52] K. De,[74] P. de Jong,[33] S.J. de Jong,[34] E. De La Cruz-Burelo,[62] C. De Oliveira Martins,[3] S. Dean,[43] J.D. Degenhardt,[62] F. Déliot,[18] M. Demarteau,[49] R. Demina,[68] P. Demine,[18] D. Denisov,[49] S.P. Denisov,[38] S. Desai,[69] H.T. Diehl,[49] M. Diesburg,[49] M. Doidge,[41] H. Dong,[69] S. Doulas,[61] L.V. Dudko,[37] L. Duflot,[16] S.R. Dugad,[29] A. Duperrin,[15] J. Dyer,[63] A. Dyshkant,[51] M. Eads,[51] D. Edmunds,[63] T. Edwards,[43] J. Ellison,[47] J. Elmsheuser,[25] V.D. Elvira,[49] S. Eno,[59] P. Ermolov,[37] O.V. Eroshin,[38] J. Estrada,[49] H. Evans,[67] A. Evdokimov,[36] V.N. Evdokimov,[38] J. Fast,[49] S.N. Fatakia,[60] L. Feligioni,[60] A.V. Ferapontov,[38] T. Ferbel,[68] F. Fiedler,[25] F. Filthaut,[34] W. Fisher,[66] H.E. Fisk,[49] I. Fleck,[23] M. Fortner,[51] H. Fox,[23] S. Fu,[49] S. Fuess,[49] T. Gadfort,[78] C.F. Galea,[34] E. Gallas,[49] E. Galyaev,[54] C. Garcia,[68] A. Garcia-Bellido,[78] J. Gardner,[56] V. Gavrilov,[36] A. Gay,[19] P. Gay,[13] D. Gelé,[19] R. Gelhaus,[47] K. Genser,[49] C.E. Gerber,[50] Y. Gershtein,[48] D. Gillberg,[5] G. Ginther,[68] T. Golling,[22] N. Gollub,[40] B. Gómez,[8] K. Gounder,[49] A. Goussiou,[54] P.D. Grannis,[69] S. Greder,[3] H. Greenlee,[49] Z.D. Greenwood,[58] E.M. Gregores,[4] Ph. Gris,[13] J.-F. Grivaz,[16] L. Groer,[67] S. Grünendahl,[49] M.W. Grünewald,[30] S.N. Gurzhiev,[38] G. Gutierrez,[49] P. Gutierrez,[72] A. Haas,[67] N.J. Hadley,[59] S. Hagopian,[48] I. Hall,[72] R.E. Hall,[46] C. Han,[62] L. Han,[7] K. Hanagaki,[49] K. Harder,[57] A. Harel,[26] R. Harrington,[61] J.M. Hauptman,[55] R. Hauser,[63] J. Hays,[52] T. Hebbeker,[21] D. Hedin,[51] J.M. Heinmiller,[50] A.P. Heinson,[47] U. Heintz,[60] C. Hensel,[56] G. Hesketh,[61] M.D. Hildreth,[54] R. Hirosky,[77] J.D. Hobbs,[69] B. Hoeneisen,[12] M. Hohlfeld,[24] S.J. Hong,[31] R. Hooper,[73] P. Houben,[33] Y. Hu,[69] J. Huang,[53] V. Hynek,[9] I. Iashvili,[47] R. Illingworth,[49] A.S. Ito,[49] S. Jabeen,[56] M. Jaffré,[16] S. Jain,[72] V. Jain,[70] K. Jakobs,[23] A. Jenkins,[42] R. Jesik,[42] K. Johns,[44] M. Johnson,[49] A. Jonckheere,[49] P. Jonsson,[42] A. Juste,[49] D. Käfer,[21] M.M. Kado,[45] S. Kahn,[70] E. Kajfasz,[15] A.M. Kalinin,[35] J. Kalk,[63] D. Karmanov,[37] J. Kasper,[60] D. Kau,[48] R. Kaur,[27] R. Kehoe,[75] S. Kermiche,[15] S. Kesisoglou,[73] A. Khanov,[68] A. Kharchilava,[54] Y.M. Kharzheev,[35] H. Kim,[74] T.J. Kim,[31] B. Klima,[49] M. Klute,[22] J.M. Kohli,[27] J.-P. Konrath,[23] M. Kopal,[72] V.M. Korablev,[38] J. Kotcher,[70] B. Kothari,[67] A. Koubarovsky,[37] A.V. Kozelov,[38] J. Kozminski,[63] A. Kryemadhi,[77] S. Krzywdzinski,[49] Y. Kulik,[49] A. Kumar,[28] S. Kunori,[59] A. Kupco,[11] T. Kurča,[20] J. Kvita,[9] S. Lager,[40] N. Lahrichi,[18] G. Landsberg,[73] J. Lazoflores,[48] A.-C. Le Bihan,[19] P. Lebrun,[20] W.M. Lee,[48] A. Leflat,[37] F. Lehner,[49,*] C. Leonidopoulos,[67] J. Leveque,[44] P. Lewis,[42] J. Li,[74] Q.Z. Li,[49] J.G.R. Lima,[51] D. Lincoln,[49] S.L. Linn,[48] J. Linnemann,[63] V.V. Lipaev,[38] R. Lipton,[49] L. Lobo,[42] A. Lobodenko,[39] M. Lokajicek,[11] A. Lounis,[19] P. Love,[41] H.J. Lubatti,[78] L. Lueking,[49] M. Lynker,[54] A.L. Lyon,[49] A.K.A. Maciel,[51] R.J. Madaras,[45] P. Mättig,[26] C. Magass,[21] A. Magerkurth,[62] A.-M. Magnan,[14] N. Makovec,[16] P.K. Mal,[29] H.B. Malbouisson,[3] S. Malik,[65] V.L. Malyshev,[35] H.S. Mao,[6] Y. Maravin,[49] M. Martens,[49] S.E.K. Mattingly,[73] A.A. Mayorov,[38] R. McCarthy,[69] R. McCroskey,[44] D. Meder,[24] A. Melnitchouk,[64] A. Mendes,[15] M. Merkin,[37] K.W. Merritt,[49] A. Meyer,[21] J. Meyer,[22] M. Michaut,[18] H. Miettinen,[76] J. Mitrevski,[67] J. Molina,[3] N.K. Mondal,[29] R.W. Moore,[5] T. Moulik,[56] G.S. Muanza,[20] M. Mulders,[49] L. Mundim,[3] Y.D. Mutaf,[69] E. Nagy,[15] M. Narain,[60] N.A. Naumann,[34] H.A. Neal,[62] J.P. Negret,[8] S. Nelson,[48] P. Neustroev,[39] C. Noeding,[23]

A. Nomerotski,[49] S.F. Novaes,[4] T. Nunnemann,[25] E. Nurse,[43] V. O'Dell,[49] D.C. O'Neil,[5] V. Oguri,[3] N. Oliveira,[3] N. Oshima,[49] G.J. Otero y Garzón,[50] P. Padley,[76] N. Parashar,[58] S.K. Park,[31] J. Parsons,[67] R. Partridge,[73] N. Parua,[69] A. Patwa,[70] G. Pawloski,[76] P.M. Perea,[47] E. Perez,[18] P. Pétroff,[16] M. Petteni,[42] R. Piegaia,[1] M.-A. Pleier,[68] P.L.M. Podesta-Lerma,[32] V.M. Podstavkov,[49] Y. Pogorelov,[54] M.-E. Pol,[2] A. Pompoš,[72] B.G. Pope,[63] W.L. Prado da Silva,[3] H.B. Prosper,[48] S. Protopopescu,[70] J. Qian,[62] A. Quadt,[22] B. Quinn,[64] K.J. Rani,[29] K. Ranjan,[28] P.A. Rapidis,[49] P.N. Ratoff,[41] S. Reucroft,[61] M. Rijssenbeek,[69] I. Ripp-Baudot,[19] F. Rizatdinova,[57] S. Robinson,[42] R.F. Rodrigues,[3] C. Royon,[18] P. Rubinov,[49] R. Ruchti,[54] V.I. Rud,[37] G. Sajot,[14] A. Sánchez-Hernández,[32] M.P. Sanders,[59] A. Santoro,[3] G. Savage,[49] L. Sawyer,[58] T. Scanlon,[42] D. Schaile,[25] R.D. Schamberger,[69] H. Schellman,[52] P. Schieferdecker,[25] C. Schmitt,[26] C. Schwanenberger,[22] A. Schwartzman,[66] R. Schwienhorst,[63] S. Sengupta,[48] H. Severini,[72] E. Shabalina,[50] M. Shamim,[57] V. Shary,[18] A.A. Shchukin,[38] W.D. Shephard,[54] R.K. Shivpuri,[28] D. Shpakov,[61] R.A. Sidwell,[57] V. Simak,[10] V. Sirotenko,[49] P. Skubic,[72] P. Slattery,[68] R.P. Smith,[49] K. Smolek,[10] G.R. Snow,[65] J. Snow,[71] S. Snyder,[70] S. Söldner-Rembold,[43] X. Song,[51] L. Sonnenschein,[17] A. Sopczak,[41] M. Sosebee,[74] K. Soustruznik,[9] M. Souza,[2] B. Spurlock,[74] N.R. Stanton,[57] J. Stark,[14] J. Steele,[58] K. Stevenson,[53] V. Stolin,[36] A. Stone,[50] D.A. Stoyanova,[38] J. Strandberg,[40] M.A. Strang,[74] M. Strauss,[72] R. Ströhmer,[25] D. Strom,[52] M. Strovink,[45] L. Stutte,[49] S. Sumowidagdo,[48] A. Sznajder,[3] M. Talby,[15] P. Tamburello,[44] W. Taylor,[5] P. Telford,[43] J. Temple,[44] M. Tomoto,[49] T. Toole,[59] J. Torborg,[54] S. Towers,[69] T. Trefzger,[24] S. Trincaz-Duvoid,[17] B. Tuchming,[18] C. Tully,[66] A.S. Turcot,[43] P.M. Tuts,[67] L. Uvarov,[39] S. Uvarov,[39] S. Uzunyan,[51] B. Vachon,[5] P.J. van den Berg,[33] R. Van Kooten,[53] W.M. van Leeuwen,[33] N. Varelas,[50] E.W. Varnes,[44] A. Vartapetian,[74] I.A. Vasilyev,[38] M. Vaupel,[26] P. Verdier,[20] L.S. Vertogradov,[35] M. Verzocchi,[59] F. Villeneuve-Seguier,[42] J.-R. Vlimant,[17] E. Von Toerne,[57] M. Vreeswijk,[33] T. Vu Anh,[16] H.D. Wahl,[48] L. Wang,[59] J. Warchol,[54] G. Watts,[78] M. Wayne,[54] M. Weber,[49] H. Weerts,[63] N. Wermes,[22] A. White,[74] V. White,[49] D. Whiteson,[45] D. Wicke,[49] D.A. Wijngaarden,[34] G.W. Wilson,[56] S.J. Wimpenny,[47] J. Wittlin,[60] M. Wobisch,[49] J. Womersley,[49] D.R. Wood,[61] T.R. Wyatt,[43] Q. Xu,[62] N. Xuan,[54] S. Yacoob,[52] R. Yamada,[49] M. Yan,[59] T. Yasuda,[49] Y.A. Yatsunenko,[35] Y. Yen,[26] K. Yip,[70] H.D. Yoo,[73] S.W. Youn,[52] J. Yu,[74] A. Yurkewicz,[69] A. Zabi,[16] A. Zatserklyaniy,[51] M. Zdrazil,[69] C. Zeitnitz,[24] D. Zhang,[49] X. Zhang,[72] T. Zhao,[78] Z. Zhao,[62] B. Zhou,[62] J. Zhu,[69] M. Zielinski,[68] D. Zieminska,[53] A. Zieminski,[53] R. Zitoun,[69] V. Zutshi,[51] and E.G. Zverev[37]

(DØ Collaboration)

[1] *Universidad de Buenos Aires, Buenos Aires, Argentina*
[2] *LAFEX, Centro Brasileiro de Pesquisas Físicas, Rio de Janeiro, Brazil*
[3] *Universidade do Estado do Rio de Janeiro, Rio de Janeiro, Brazil*
[4] *Instituto de Física Teórica, Universidade Estadual Paulista, São Paulo, Brazil*
[5] *University of Alberta, Edmonton, Alberta, Canada, Simon Fraser University, Burnaby, British Columbia, Canada, York University, Toronto, Ontario, Canada, and McGill University, Montreal, Quebec, Canada*
[6] *Institute of High Energy Physics, Beijing, People's Republic of China*
[7] *University of Science and Technology of China, Hefei, People's Republic of China*
[8] *Universidad de los Andes, Bogotá, Colombia*
[9] *Center for Particle Physics, Charles University, Prague, Czech Republic*
[10] *Czech Technical University, Prague, Czech Republic*
[11] *Center for Particle Physics, Institute of Physics, Academy of Sciences of the Czech Republic, Prague, Czech Republic*
[12] *Universidad San Francisco de Quito, Quito, Ecuador*
[13] *Laboratoire de Physique Corpusculaire, IN2P3-CNRS, Université Blaise Pascal, Clermont-Ferrand, France*
[14] *Laboratoire de Physique Subatomique et de Cosmologie, IN2P3-CNRS, Universite de Grenoble 1, Grenoble, France*
[15] *CPPM, IN2P3-CNRS, Université de la Méditerranée, Marseille, France*
[16] *IN2P3-CNRS, Laboratoire de l'Accélérateur Linéaire, Orsay, France*
[17] *LPNHE, IN2P3-CNRS, Universités Paris VI and VII, Paris, France*
[18] *DAPNIA/Service de Physique des Particules, CEA, Saclay, France*
[19] *IReS, IN2P3-CNRS, Université Louis Pasteur, Strasbourg, France, and Université de Haute Alsace, Mulhouse, France*
[20] *Institut de Physique Nucléaire de Lyon, IN2P3-CNRS, Université Claude Bernard, Villeurbanne, France*
[21] *III. Physikalisches Institut A, RWTH Aachen, Aachen, Germany*
[22] *Physikalisches Institut, Universität Bonn, Bonn, Germany*
[23] *Physikalisches Institut, Universität Freiburg, Freiburg, Germany*
[24] *Institut für Physik, Universität Mainz, Mainz, Germany*
[25] *Ludwig-Maximilians-Universität München, München, Germany*
[26] *Fachbereich Physik, University of Wuppertal, Wuppertal, Germany*
[27] *Panjab University, Chandigarh, India*
[28] *Delhi University, Delhi, India*
[29] *Tata Institute of Fundamental Research, Mumbai, India*
[30] *University College Dublin, Dublin, Ireland*

[31] Korea Detector Laboratory, Korea University, Seoul, Korea
[32] CINVESTAV, Mexico City, Mexico
[33] FOM-Institute NIKHEF and University of Amsterdam/NIKHEF, Amsterdam, The Netherlands
[34] Radboud University Nijmegen/NIKHEF, Nijmegen, The Netherlands
[35] Joint Institute for Nuclear Research, Dubna, Russia
[36] Institute for Theoretical and Experimental Physics, Moscow, Russia
[37] Moscow State University, Moscow, Russia
[38] Institute for High Energy Physics, Protvino, Russia
[39] Petersburg Nuclear Physics Institute, St. Petersburg, Russia
[40] Lund University, Lund, Sweden, Royal Institute of Technology and Stockholm University, Stockholm, Sweden, and Uppsala University, Uppsala, Sweden
[41] Lancaster University, Lancaster, United Kingdom
[42] Imperial College, London, United Kingdom
[43] University of Manchester, Manchester, United Kingdom
[44] University of Arizona, Tucson, Arizona 85721, USA
[45] Lawrence Berkeley National Laboratory and University of California, Berkeley, California 94720, USA
[46] California State University, Fresno, California 93740, USA
[47] University of California, Riverside, California 92521, USA
[48] Florida State University, Tallahassee, Florida 32306, USA
[49] Fermi National Accelerator Laboratory, Batavia, Illinois 60510, USA
[50] University of Illinois at Chicago, Chicago, Illinois 60607, USA
[51] Northern Illinois University, DeKalb, Illinois 60115, USA
[52] Northwestern University, Evanston, Illinois 60208, USA
[53] Indiana University, Bloomington, Indiana 47405, USA
[54] University of Notre Dame, Notre Dame, Indiana 46556, USA
[55] Iowa State University, Ames, Iowa 50011, USA
[56] University of Kansas, Lawrence, Kansas 66045, USA
[57] Kansas State University, Manhattan, Kansas 66506, USA
[58] Louisiana Tech University, Ruston, Louisiana 71272, USA
[59] University of Maryland, College Park, Maryland 20742, USA
[60] Boston University, Boston, Massachusetts 02215, USA
[61] Northeastern University, Boston, Massachusetts 02115, USA
[62] University of Michigan, Ann Arbor, Michigan 48109, USA
[63] Michigan State University, East Lansing, Michigan 48824, USA
[64] University of Mississippi, University, Mississippi 38677, USA
[65] University of Nebraska, Lincoln, Nebraska 68588, USA
[66] Princeton University, Princeton, New Jersey 08544, USA
[67] Columbia University, New York, New York 10027, USA
[68] University of Rochester, Rochester, New York 14627, USA
[69] State University of New York, Stony Brook, New York 11794, USA
[70] Brookhaven National Laboratory, Upton, New York 11973, USA
[71] Langston University, Langston, Oklahoma 73050, USA
[72] University of Oklahoma, Norman, Oklahoma 73019, USA
[73] Brown University, Providence, Rhode Island 02912, USA
[74] University of Texas, Arlington, Texas 76019, USA
[75] Southern Methodist University, Dallas, Texas 75275, USA
[76] Rice University, Houston, Texas 77005, USA
[77] University of Virginia, Charlottesville, Virginia 22901, USA
[78] University of Washington, Seattle, Washington 98195, USA

(Dated: May 26, 2005)

We present a measurement of the top quark pair ($t\bar{t}$) production cross section in $p\bar{p}$ collisions at $\sqrt{s} = 1.96$ TeV using events with two charged leptons in the final state. This analysis utilizes an integrated luminosity of 224-243 pb^{-1} collected with the DØ detector at the Fermilab Tevatron Collider. We observe 13 events in the e^+e^-, $e\mu$ and $\mu^+\mu^-$ channels with an expected background of 3.2 ± 0.7 events. For a top quark mass of 175 GeV, we measure a $t\bar{t}$ production cross section of $\sigma_{t\bar{t}} = 8.6^{+3.2}_{-2.7}(\text{stat}) \pm 1.1(\text{syst}) \pm 0.6(\text{lumi})$ pb, consistent with the standard model prediction.

PACS numbers: 13.85.Lg, 13.85.Qk, 14.65.Ha

The top quark was discovered [1] in 1995 at the Fermilab Tevatron Collider in $p\bar{p}$ collisions at $\sqrt{s} = 1.8$ TeV. Its observation completed the third quark weak isospin doublet suggested by the absence of flavor changing neu-

tral current interactions [2] and measurement of the b quark weak isospin [3]. By virtue of its large mass ($m_t = 178.0 \pm 4.3$ GeV [4]), the top quark could decay into exotic particles, e.g. a charged Higgs boson [5]. Such decays would lead to a measured $t\bar{t}$ production cross section ($\sigma_{t\bar{t}}$) apparently dependent on the $t\bar{t}$ final state. It is therefore necessary to precisely measure $\sigma_{t\bar{t}}$ in all decay channels and compare it with the standard model prediction. The increased luminosity and higher collision energy of $\sqrt{s} = 1.96$ TeV at the Run II of Tevatron permit substantially more accurate measurement of $\sigma_{t\bar{t}}$ in all final states.

In the $SU(2) \times U(1)$ electroweak model with one Higgs doublet [6], each top quark of a $t\bar{t}$ pair is expected to decay approximately 99.8% of the time to a W boson and a b quark [7]. Dilepton final states arise when both W bosons decay leptonically. These occur along with two energetic jets resulting from the hadronization of the b quarks and missing transverse energy ($\not\!\!E_T$) from the high transverse momentum (p_T) neutrinos. In this Letter, we present a measurement of $\sigma_{t\bar{t}}$ with 224-243 pb^{-1} of $p\bar{p}$ collider data at $\sqrt{s} = 1.96$ TeV collected with the upgraded DØ detector [8]. We consider the e^+e^-, $e\mu$ and $\mu^+\mu^-$ final states. The electrons and muons may originate either directly from a W boson or indirectly from a $W \to \tau\nu$ decay. The corresponding $t\bar{t}$ branching fractions (B) are 1.58%, 3.16%, and 1.57% [7] for the e^+e^-, $e\mu$, and $\mu^+\mu^-$ channels, respectively.

The DØ detector has a silicon microstrip tracker and a central fiber tracker located within a 2 T superconducting solenoidal magnet [8]. The surrounding liquid-argon/uranium calorimeter has a central cryostat covering pseudo-rapidities $|\eta|$ up to 1.1 [9], and two end cryostats extending coverage to $|\eta| \approx 4$ [10]. A muon system [11] resides beyond the calorimetry, and consists of a layer of tracking detectors and scintillation trigger counters before 1.8 T toroids, followed by two similar layers after the toroids. Luminosity is measured using plastic scintillator arrays located in front of the end cryostats. The trigger and data acquisition systems are designed to accommodate the high luminosities of Run II. The data used in this analysis were collected by requiring two leptons (e or μ) in the hardware trigger and one or two leptons in the software triggers [8].

To extract the $t\bar{t}$ signal, we select events with two high-p_T isolated leptons, large $\not\!\!E_T$, and at least two jets. We further improve the signal to background ratio by selecting events with kinematics compatible with $t\bar{t}$ events. To derive the cross section we determine the overall efficiency ϵ (including trigger, geometrical, and event selection efficiencies) for $t\bar{t}$ and the number of expected background events. We distinguish two categories of backgrounds: "physics" and "instrumental". Physics backgrounds are processes in which the charged leptons arise from electroweak boson decays and the $\not\!\!E_T$ originates from high p_T neutrinos. This signature arises in $Z/\gamma^* \to \tau^+\tau^-$ where the τ leptons decay leptonically, and WW/WZ (diboson) production. Instrumental backgrounds are defined as events in which (a) a jet or a lepton within a jet fakes the isolated lepton signature, or (b) the $\not\!\!E_T$ originates from misreconstructed jet or lepton energies or from noise in the calorimeter.

The electrons used in the analysis are defined as clusters of calorimeter cells for which (a) the fraction of energy deposited in the electromagnetic section of the calorimeter has to be at least 90% of the total cluster energy, (b) the energy is concentrated in a narrow cone and isolated from further calorimeter energy, (c) the shape of the shower is compatible with that of an electron, (d) the electron matches a charged track in the tracking system. In order to further remove backgrounds we use (e) a discriminant that selects prompt isolated electrons based on the tracking system and calorimeter information [12]. Electrons which fulfill criteria (a) to (e) are referred to as "tight" electrons. For background calculations we introduce "loose" electrons for which only (a) and (b) are required. The muons considered in the analysis are defined as tracks reconstructed in the three layers of the muon system, with a matching track in the tracking system. The energy deposited in the calorimeter inside a hollow cone around the muon must be less than 12% of the muon p_T. To further remove background, the sum of the charged track momenta in a cone around the muon track has to be smaller than 12% of the muon p_T. Muons that fulfill all these criteria are referred to as "tight" muons. For background calculations, we introduce "loose" muons for which the isolation criteria are relaxed.

Jets are reconstructed with a fixed cone of radius $\Delta\mathcal{R} = 0.5$ [13] and must be confirmed by the independent calorimeter trigger readout. Jet energy calibration is applied to the jets [14]. The $\not\!\!E_T$ is equal in magnitude and opposite in direction to the vector sum of all significant calorimeter cell transverse energies. It is corrected for the transverse momenta of all isolated muons, as well as for the corrections to the electron and jet energies.

Event selections for each channel are optimized to minimize the expected statistical uncertainty on the cross section. We select events with at least two jets with $p_T^j > 20$ GeV and $|y| < 2.5$ [9] and two leptons with $p_T^\ell > 15$ GeV. Muons are accepted in the region $|\eta| < 2.0$, while electrons must be within $|\eta| < 1.1$ or $1.5 < |\eta| < 2.5$. The two leptons are required to be of opposite signs in the e^+e^- and $\mu^+\mu^-$ channels.

A cut on $\not\!\!E_T$ is crucial to reduce the otherwise large Z/γ^* background. This background is particularly severe in the e^+e^- and $\mu^+\mu^-$ channels. Due to different resolutions in electron energies and muon momenta, the optimization leads to different selections in the three channels. In the $e\mu$ channel, we require $\not\!\!E_T > 25$ GeV and $\Delta\phi(\not\!\!E_T, \mu) > 0.25$, where $\Delta\phi(\not\!\!E_T, \mu)$ is the azimuthal angle between the $\not\!\!E_T$ and the muon. The latter gives additional rejection against $Z/\gamma^* \to \tau\tau$ background in events

with two jets. In the e^+e^- channel, we veto events with dielectron invariant mass $80 \leq M_{ee} \leq 100$ GeV and require $\not\!\!E_T > 35$ GeV ($\not\!\!E_T > 40$ GeV) for $M_{ee} > 100$ GeV ($M_{ee} < 80$ GeV). In the $\mu^+\mu^-$ channel, we accept events with $\not\!\!E_T > 35$ GeV. This cut is tightened at low and high values of $\Delta\phi(\not\!\!E_T, \mu_1)$ where μ_1 denotes the leading p_T muon. Events with $\Delta\phi(\not\!\!E_T, \mu_1) > 175°$ are removed.

The final selection in the $e\mu$ channel requires $H_T^\ell = p_T^{\ell_1} + \Sigma(p_T^j) > 140$ GeV, where $p_T^{\ell_1}$ denotes the p_T of the leading lepton. This cut effectively rejects the largest backgrounds for this final state which arise from $Z/\gamma^* \to \tau^+\tau^-$ and diboson production. The e^+e^- analysis uses a cut on sphericity $\mathcal{S} = 3(\epsilon_1 + \epsilon_2)/2 > 0.15$, where ϵ_1 and ϵ_2 are the two leading eigenvalues of the normalized momentum tensor [15]. This requirement rejects events in which jets are produced in a planar geometry through gluon radiation. The final selection applied in the $\mu^+\mu^-$ channel further rejects the $Z/\gamma^* \to \mu^+\mu^-$ background. We compute for each $\mu^+\mu^-$ event the χ^2 of a fit to the $Z \to \mu^+\mu^-$ hypothesis given the measured muon momenta and known resolutions. Selecting events with $\chi^2 > 2$ is more effective than selecting on the dimuon invariant mass for this channel.

Signal acceptances and efficiencies are derived from a combination of Monte Carlo simulation (MC) and data. Top quark pair production is simulated using ALPGEN [16] with $m_t = 175$ GeV. PYTHIA [17] is used for fragmentation and decay. B hadron and τ lepton decays are modeled via EVTGEN [18] and TAUOLA [19], respectively. A full detector simulation using GEANT [20] is performed. Lepton trigger and identification efficiencies as well as lepton momentum resolutions are derived from $Z/\gamma^* \to \ell^+\ell^-$ ($\ell = e, \mu$) data. These per-lepton normalization factors and momentum smearings are applied to MC events to ensure the simulated samples provide an accurate description of the data. The jet reconstruction efficiency, jet energy resolution and $\not\!\!E_T$ resolution in the MC are adjusted to their measured values in data.

To calculate the expected number of events from physics backgrounds, we use $Z/\gamma^* \to \tau^+\tau^-$ and diboson MC samples generated with PYTHIA and ALPGEN, respectively. The $Z/\gamma^* \to \tau^+\tau^-$ contribution is normalized to the cross section measured by DØ [21]. For the diboson processes, diboson + 2 jets events are generated at leading order (LO) and are scaled by the ratio of the next-to-leading order to LO inclusive cross sections derived for diboson inclusive production [22].

Instrumental backgrounds are determined from the data. Fake electrons can arise from jets comprised essentially of a leading π^0/η and an overlapping or conversion-produced track. We estimate this background by calculating the fraction f_e of loose electrons which appear as tight electrons in a control sample dominated by fake electrons. In the e^+e^- channel the control sample consists of events that satisfied the trigger and have two loose electrons. In the $e\mu$ channel the events in the control sample must satisfy the trigger and have one tight muon and one loose electron. Contributions from processes with real electrons ($W \to e\nu$ and $Z/\gamma^* \to e^+e^-$) are suppressed by requiring $\not\!\!E_T < 10$ GeV in both e^+e^- and $e\mu$ channels and $|M_{ee} - M_Z| > 15$ GeV in the e^+e^- channel only. We also veto events in which both loose electrons have a matching track. We observe that f_e measured in the e^+e^- and $e\mu$ control samples agree within statistical errors. The predicted number of events with a fake electron in the final sample is obtained by multiplying the number of e^+e^- ($e\mu$) events with one loose electron and one tight electron (muon) by f_e.

An isolated muon can be mimicked by a muon in a jet when the jet is not reconstructed. We measure the fraction f_μ of loose muons that satisfy the tight muon criteria in a control sample dominated by fake muons. In the $\mu^+\mu^-$ channel the control sample is defined as events that have two loose muons. To suppress physics processes with real isolated muons the leading p_T muon is required to fail the tight muon criteria. This cuts efficiently $Z/\gamma^* \to \mu^+\mu^-$ events but also $W \to \mu\nu$ events where a second-leading muon might arise from a muon in a jet. The number of events with a fake muon contributing to the final sample is estimated by counting the number of events with one tight muon and a loose muon and multiplying it by f_μ. In the $e\mu$ channel the contribution from events where both leptons are fake leptons is already accounted for by using f_e. The remaining contribution from events with a real electron and a fake muon, is determined by combining f_e and a fake rate f_μ obtained on a control sample that satisfies the $e\mu$ trigger.

The processes $Z/\gamma^* \to \ell^+\ell^-$ ($\ell = e, \mu$), while lacking high p_T neutrinos, might have a significant amount of measured $\not\!\!E_T$ due to limited $\not\!\!E_T$ resolution. In the e^+e^- channel, this background is estimated by measuring a $\not\!\!E_T$ misreconstruction rate on data and applying it to the simulation. We observe that the $\not\!\!E_T$ spectrum in e^+e^- events with $80 \leq M_{ee} \leq 100$ GeV agrees well with the $\not\!\!E_T$ spectrum observed in $\gamma + 2$ jets candidate events. We obtain the $\not\!\!E_T$ misreconstruction rate in data as the ratio of the number of $\gamma + 2$ jets events passing the $\not\!\!E_T$ selection divided by the number failing the selection. The $\not\!\!E_T$ misreconstruction rate is also consistent with $Z/\gamma^* \to e^+e^- + 2$ jets simulation. This rate is multiplied by the number of events that fail the $\not\!\!E_T$ selections but pass all other selections. In the $\mu^+\mu^-$ channel, the expected contribution of $Z/\gamma^* \to \mu^+\mu^-$ background in the final sample is derived from events simulated with ALPGEN. Good agreement is observed between the data and the simulation in the variables $\not\!\!E_T$ and $\Delta\phi(\not\!\!E_T, \mu_1)$. This allows us to obtain the probability for a $Z/\gamma^* \to \mu^+\mu^-$ event to pass the $\not\!\!E_T$ selection from the simulation. The sample is normalized to the number of observed $Z/\gamma^* \to \mu^+\mu^-$ events in the data with $70 \leq M_{\mu\mu} \leq 110$ GeV before the $\not\!\!E_T$ selection.

The number of observed events and estimated physics

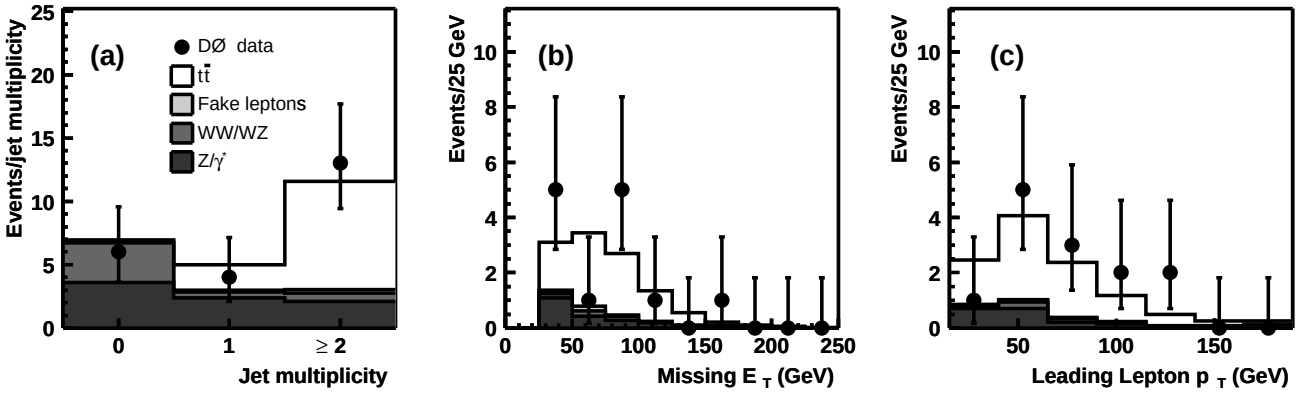

FIG. 1: Predicted and observed (a) number of events with 0, 1 and 2 or more jets with all other selections applied, (b) $\not\!\!E_T$ and (c) leading lepton p_T in dilepton events after all selections. The Z/γ^* contribution includes e^+e^-, $\tau^+\tau^- \to e\mu$, and $\mu^+\mu^-$ final states. The $t\bar{t}$ prediction is shown for $\sigma_{t\bar{t}} = 7$ pb.

and instrumental backgrounds in the dilepton + 2 jets sample, the integrated luminosities and the $\epsilon \times B$ for the $t\bar{t}$ signal are given in Table I for each channel. We observe 5, 8 and 0 events in the e^+e^-, $e\mu$ and $\mu^+\mu^-$ channels, respectively. We estimate the probability to observe ≥ 5, ≥ 8, and exactly 0 events in the e^+e^-, $e\mu$, and $\mu^+\mu^-$ channels as 22%, 43%, and 5%, respectively, using the measured $\sigma_{t\bar{t}}$ and taking into account systematic uncertainties. By generating pseudo-experiments we estimate that 20% of the possible outcomes have lower likelihoods than that of our observation. The significance of the observed $t\bar{t}$ signal over the background is 3.8 standard deviations.

To compute the cross section, we calculate in each channel the probability to observe the number of events seen in the data as a function of $\sigma_{t\bar{t}}$ given the number of background events and the signal efficiencies. The combined cross section is the value of $\sigma_{t\bar{t}}$ that maximizes the product of the likelihoods in the three channels. The resulting top quark pair production cross section at $\sqrt{s} = 1.96$ TeV in dilepton final states is

$$\sigma_{t\bar{t}} = 8.6^{+3.2}_{-2.7}(\text{stat}) \pm 1.1(\text{syst}) \pm 0.6(\text{lumi}) \text{ pb}$$

for $m_t = 175$ GeV, within errors of the standard model theoretical prediction of 6.77 ± 0.42 pb [23] and in agreement with the recent result in Ref. [24]. We find $\sigma_{t\bar{t}}$ also consistent with measurements carried out in different final states [12, 25]. The total systematic uncertainty is obtained by varying the background prediction and signal efficiencies within their uncertainties and taking into account correlations. The dominant systematic uncertainties are given in Table II. In addition a 6.5% systematic uncertainty is assigned to the luminosity measurement [26]. The top quark mass affects the signal efficiency, resulting in a dependence of $\sigma_{t\bar{t}}$ on m_t given by $d\sigma_{t\bar{t}}/dm_t = -0.08$ pb/GeV for m_t in the range 160 GeV to 190 GeV.

Figure 1(a) shows that the observed number of events with 0, 1, and 2 or more jets, with all other selections applied, is consistent with the prediction (assuming $\sigma_{t\bar{t}} = 7$ pb). Figure 1(b) shows that the observed and predicted $\not\!\!E_T$ spectra after all selections agree well. Other kinematic distributions in dilepton events are also well described by the sum of $t\bar{t}$ signal and background contributions at various steps of the event selection.

The leading lepton p_T spectrum in the $t\bar{t}$ dilepton final states has recently been studied by the CDF Collaboration [27] and a mild excess has been observed at low transverse momenta. This is not confirmed by our data, as shown in Fig. 1(c). To test agreement between data and the prediction, we generate pseudo-experiments from the predicted leading lepton p_T spectrum and use our measured $\sigma_{t\bar{t}}$ to normalize the $t\bar{t}$ signal. We find that 31% of the pseudo-experiments are less consistent with the parent distribution than the data. We conclude that data agree well with the prediction.

In summary, we have measured the top quark pair production cross section at $\sqrt{s} = 1.96$ TeV in e^+e^-, $e\mu$ and $\mu^+\mu^-$ final states to be $\sigma_{t\bar{t}} = 8.6^{+3.2}_{-2.7}(\text{stat}) \pm 1.1(\text{syst}) \pm 0.6(\text{lumi})$ pb for $m_t = 175$ GeV, in agreement with the standard model prediction and with measurements in other final states.

We thank the staffs at Fermilab and collaborating institutions, and acknowledge support from the DOE and NSF (USA); CEA and CNRS/IN2P3 (France); FASI, Rosatom and RFBR (Russia); CAPES, CNPq, FAPERJ, FAPESP and FUNDUNESP (Brazil); DAE and DST (India); Colciencias (Colombia); CONACyT (Mexico); KRF (Korea); CONICET and UBACyT (Argentina); FOM (The Netherlands); PPARC (United Kingdom); MSMT (Czech Republic); CRC Program, CFI, NSERC and WestGrid Project (Canada); BMBF and DFG (Germany); SFI (Ireland); Research Corporation, Alexander von Humboldt Foundation, and the Marie Curie Pro-

TABLE I: Expected signal (assuming $m_t = 175$ GeV and $\sigma_{t\bar{t}} = 7$ pb) and background event yields for e^+e^-, $e\mu$, and $\mu^+\mu^-$ channels. Instrumental backgrounds include $\not\!\!E_T$ and fake lepton backgrounds. Total uncertainties are given.

Channel	e^+e^-	$e\mu$	$\mu^+\mu^-$
Integrated luminosity (pb^{-1})	243	228	224
Physics backgrounds	0.3 ± 0.1	0.7 ± 0.2	0.2 ± 0.1
Instrumental backgrounds	0.7 ± 0.1	0.2 ± 0.1	$1.1^{+0.4}_{-0.3}$
Total background	0.9 ± 0.1	0.9 ± 0.2	1.4 ± 0.4
$\epsilon \times B$ (10^{-3})	$1.1^{+0.1}_{-0.2}$	$3.2^{+0.4}_{-0.3}$	1.0 ± 0.1
Expected signal	$1.9^{+0.2}_{-0.3}$	$5.1^{+0.6}_{-0.5}$	1.6 ± 0.2
Total prediction	2.8 ± 0.3	$6.1^{+0.6}_{-0.5}$	2.9 ± 0.6
Observed	5	8	0

TABLE II: Summary of systematic uncertainties on $\sigma_{t\bar{t}}$.

Source	$\Delta\sigma_{t\bar{t}}$ (pb)
Jet energy calibration	$+0.8\ -0.7$
Jet identification	$+0.3\ -0.6$
Muon identification	$+0.5\ -0.4$
Electron identification	± 0.3
Trigger	$+0.3\ -0.2$
Other	$+0.2\ -0.3$
Total	± 1.1

gram.

[*] Visitor from University of Zurich, Zurich, Switzerland.

[1] CDF Collaboration, F. Abe *et al.*, Phys. Rev. Lett. **74**, 2626 (1995); DØ Collaboration, S. Abachi *et al.*, Phys. Rev. Lett. **74**, 2632 (1995).

[2] A. Bean *et al.*, Phys. Rev. D **35**, 3533 (1987).

[3] E. Elsen *et al.*, Z. Physik C **46**, 349 (1990); H. Behrend *et al.*, Z. Physik C **47**, 333 (1990); A. Shimonaka *et al.*, Phys. Lett. B **268**, 457 (1991).

[4] CDF and DØ collaborations, TEVEWWG, hep-ex/0404010.

[5] J.F. Gunion *et al.*, *The Higgs Hunters Guide* (Addison-Wesley, Redwood City, California, 1990), p. 200.

[6] A. Salam, *Elementary Particle Theory* (Stockholm, Almquist and Wiksells, 1967); S. Weinberg, Phys. Rev. Lett. **19**, 1264 (1967).

[7] S. Eidelman *et al.*, Phys. Lett. B **592**, 1 (2004).

[8] DØ Collaboration, V. Abazov *et al.*, "The Upgraded DØ Detector," in preparation for submission. to Nucl. Instrum. Meth. Phys. Res. A.

[9] Rapidity y and pseudo-rapidity η are defined as functions of the polar angle θ and parameter β as $y(\theta,\beta) \equiv \frac{1}{2}\ln[(1+\beta\cos\theta)/(1-\beta\cos\theta)]$; $\eta(\theta) \equiv y(\theta,1)$, where β is the ratio of a particle's momentum to its energy.

[10] DØ Collaboration, S. Abachi *et al.*, Nucl. Instrum. Methods Phys. Res. A **338**, 185 (1994).

[11] V. Abazov *et al.*, FERMILAB-PUB-05-034-E (2005)

[12] DØ Collaboration, V. Abazov *et al.*, hep-ex/0504043.

[13] Jets are defined using the iterative seed-based cone algorithm with $\Delta\mathcal{R} = \sqrt{(\Delta\phi)^2 + (\Delta\eta)^2} = 0.5$ (where ϕ is the azimuthal angle), including mid-points as described in Sec. 3.5 (p. 47) of G. C. Blazey *et al.*, in *Proceedings of the Workshop: "QCD and Weak Boson Physics in Run II,"* edited by U. Baur, R. K. Ellis, and D. Zeppenfeld, FERMILAB-PUB-00-297 (2000).

[14] DØ Collaboration, B. Abbott *et al.*, Nucl. Instrum. Meth. A **424**, 352 (1999).

[15] V. Barger, J. Ohnemus, and R. J. N. Phillips, Phys. Rev. D **48**, 3953 (1993).

[16] M. L. Mangano *et al.*, JHEP **07**,001 (2003).

[17] T. Sjöstrand *et al.*, Comput. Phys. Commun. **135**, 238 (2001).

[18] D. J. Lange, Nucl. Instrum. Methods Phys. Res. A **462**, 152 (2001).

[19] S. Jadach *et al.*, Comp. Phys. Commun. **76**, 361 (1993).

[20] R. Brun and F. Carminati, CERN Program Library Long Writeup W5013, 1993 (unpublished).

[21] DØ Collaboration, V. Abazov *et al.*, Phys. Rev. D **71**, 072004 (2005).

[22] J. M. Campbell and R. K. Ellis, Phys. Rev. D **60**, 113006 (1999).

[23] R. Bonciani *et al.*, Nucl. Phys. **B529**, 424 (1998); N. Kidonakis and R. Vogt, Phys. Rev. D **68**, 114014 (2003); M. Cacciari *et al.*, JHEP **404**, 68 (2004).

[24] CDF Collaboration, D. Acosta *et al.*, Phys. Rev. Lett. **93**, 142001 (2004).

[25] CDF Collaboration, D. Acosta *et al.*, Phys. Rev. D **71**, 052003 (2005); CDF Collaboration, D. Acosta *et al.*, Phys. Rev. D **71**, 072005 (2005); DØ Collaboration, V. Abazov *et al.*, hep-ex/0504058; CDF Collaboration, D. Acosta *et al.*, hep-ex/0504053.

[26] T. Edwards *et al.*, FERMILAB-TM-2278-E (2004).

[27] CDF Collaboration, D. Acosta *et al.*, hep-ex/0412042.